Modeling Internal Solitary Wave Development at the Head of a Submarine Canyon

Timothy F. Duda, Weifeng Gordon Zhang, Karl R. Helfrich,
Ying-Tsong Lin and Arthur E. Newhall

Woods Hole Oceanographic Institution
tduda@whoi.edu

Abstract

Groups of nonlinear internal waves observed near submarine canyons exhibit location and direction features that we seek to explain. Notably, waves move to the right when looking up a boreal canyon and radiate from a compact apparent source. We have modeled and explained features of the underlying internal tide that is locally generated as surface tidal waves move over the slopes, and here we move on to the short-scale nonlinear waves that co-exist with the internal tide. Two-dimensional nonlinear wave modeling with the extended rotation-modified Korteweg DeVries equation nested into the internal-tide fields produces short (nonhydrostatic) waves that qualitatively agree with observations. Full three-dimensional non-hydrostatic modeling of the tidal response with MITgcm produced short waves that mimic observations, and the results are used to diagnose the causes of localization and directionality. A multiple-scattering approach of a single normal mode can explain the internal-tide signature, but is likely insufficient for the full wave field.

1 Introduction

Nonlinear internal waves are known to be widespread throughout the ocean, thanks to their being detectable with satellite sensors, and a compilation by Jackson (2004) shows some remarkable images. These waves can be caused by flow over bathymetric features or by oscillatory flows over slopes. For subcritical barotropic tidal flow over topography, where the flow speed is less than speed of the radiating waves, the response is often an intermediate wave, a long-wavelength internal tide (Baines (1982), Garrett and Kunze (2007)). The internal tide (IT) waves can steepen by the effects of nonlinearity and often develop into nonlinear wave groups, see e.g. Li and Farmer (2011). Many theoretical and computational modeling studies have explained the details of the processes, which can vary greatly over the wide variety of parameter regimes that are found in the worlds oceans. Here we study nonlinear wave packet generation from barotropic internal tidal flow incident on canyons that can incise the outer edge of the continental shelf. Two methods are used: the MITgcm dynamical ocean model that includes the effects of non-hydrostatic pressure, and a hybrid modeling approach the can be used for more rapid computations but has recognized limitations.

A number of satellite synthetic aperture radar images show nonlinear wave packets moving to the right from the head of canyons, when looking up a boreal canyon. Figure 1 shows this phenomenon. In prior work, we used both a computational ocean model with only hydrostatic pressure and a normal-mode based wave propagation model to explain the geometry of the internal tide beam apparently responsible for the waves in the figure (Zhang et al. (2014)). This success motivated continued work to explain the actual nonlinear wave packet like the one moving northward in the figure, building on the explanation of the underlying IT.

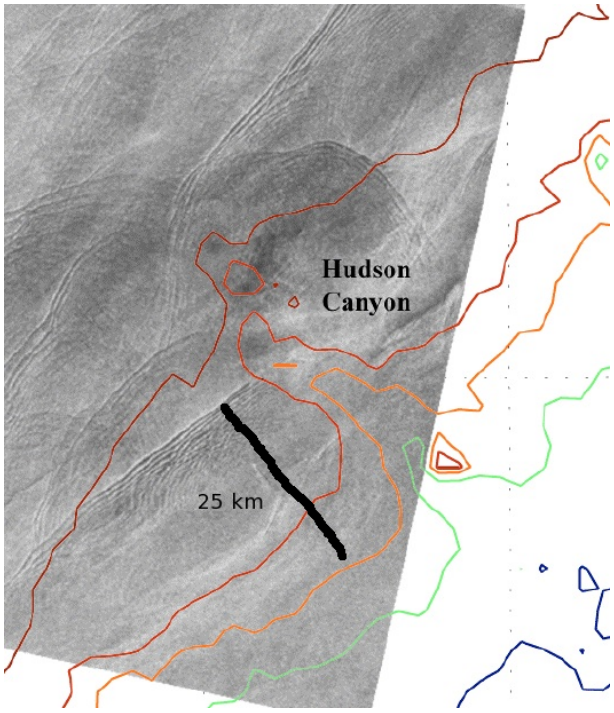

Figure 1: Internal waves are seen to be moving away from and to the right (northward) of Hudson Canyon near New York, when looking up the canyon. The waves are directly above the Hudson Canyon label. The light and dark bands in this synthetic aperture radar image show leading and trailing edges of mode-one internal waves (areas of convergent and divergent surface flow, respectively, for mode-one waves of depression) of order 500-m typical wavelength. Image adapted from (Jackson (2004)). Depth contours, from shallow at upper left: 100 m, 200 m, 500 m, 1000 m, 2000 m.

2 Multiple Scattering of Tides at Slopes

The canyon internal tide response paper by Zhang et al. (2014) identified scenarios to explain asymmetric internal tides at symmetric canyons. Figure 2 shows asymmetric internal tides generated using a computational model. The computation was made with the ROMS modeling system (Shchepetkin and McWilliams (2005)) and used the hydrostatic pressure approximation. Matching the computational results with semi-analytical model results relied upon an argument that the barotropic to baroclinic energy conversion process was stronger on the right side of the canyon (looking up) than on the left side. The variation of the direction of seabed height gradient across the canyon is responsible for the formation of beams, as determined by the semi-analytical model, with no spatial variations of the conversion rate needed. However, the relative strengths of the beams in the semi-analytic model do not match the computations unless this adjustment is made to the effective conversion rate in the semi-analytic model. Because the slopes are symmetric about the canyon axis, and the barotropic tidal currents are the same, the following multiple scattering process was put forth as an explanation.

An approximate solution of the full response to a surface tide forcing is given by the second order Born approximation. The full field is given by

$$\Phi(x,y) = \Phi_0(x,y) + \int G(x,y,x',y')C(x',y')\Phi(x',y')dx'dy' \qquad (1)$$

where Φ_0 is the barotropic tidal field, G is the Green's function of a propagating response, and C is the internal tide conversion coefficient. The standard Born approximation (single-

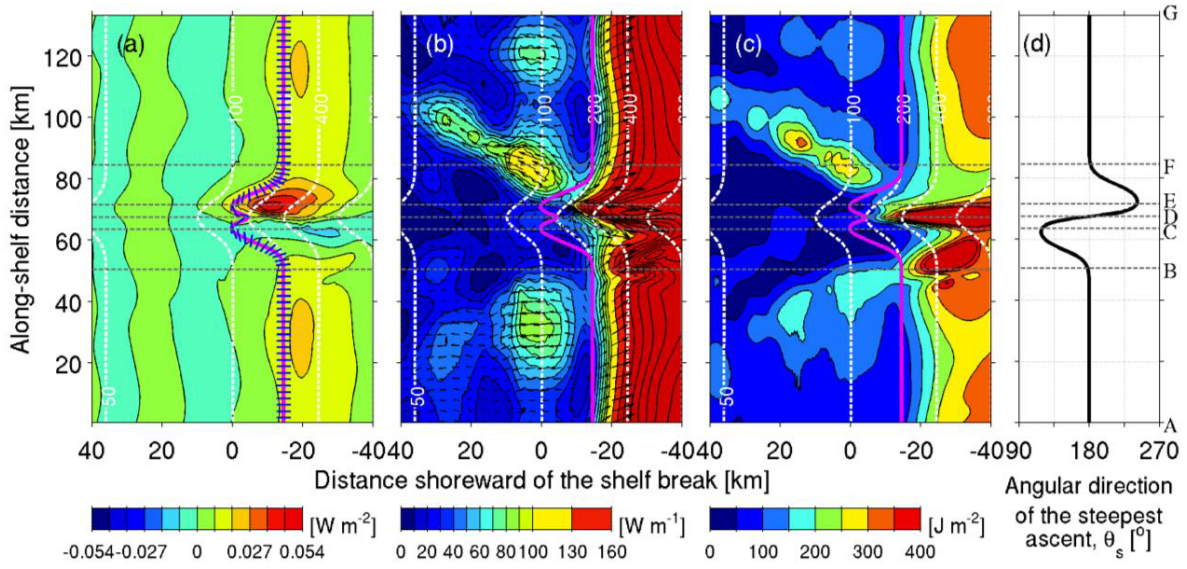

Figure 2: Internal tides moving away and to the right in the tidally-forced ROMS modeling are shown in this figure from Zhang et al. (2014). Shown are (a) vertically integrated barotropic-to-baroclinic energy conversion rate C, (b) baroclinic energy flux (color depicts magnitude), (c) vertically-integrated baroclinic (internal wave) kinetic energy density, and (d) the direction of the steepest ascent along the critical-slope locus (also drawn in (a) with short blue lines). The locus is shown with magenta lines in (a)-(c).

scatter model) is $\Phi_B(x,y) = \Phi_0 + \int GC\Phi_0 dx'dy'$. The second-order model (Schiff (1968)) is

$$\Phi_2 = \Phi_0 + \int G(x,y,x',y')C(x',y')\Phi_B(x',y')dx'dy' \tag{2}$$

We have not built analytical 2nd order solutions using this expression. However, Zhang et al. (2014) show that the phase advance of a mode-one internal tide along the locus $L(x,y)$ of seafloor critical slope (wavenumber $k = d\theta/dx$) is very similar to the phase advance of the forcing along L. This sensitivity of the full response to propagating scattered waves (mode-one internal tide in this case) offers an explanation of enhanced internal tide forcing and stronger beam response on one side of a canyon (asymmetric generation) when the barotropic tide (Ψ_0 in this case) is symmetric and C is only weakly spatially variable or constant. The inability of the single-scatter model to include different effective conversions of barotropic energy to baroclinic energy on the opposite sides of the canyon (as opposed to differing C) supports the multiple-scattering explanation.

3 Nonhydrostatic Computational Model of the Wave Response

A model that doesn't invoke the hydrostatic pressure assumption is required to model the nonlinear wave response to the tidal flow. The MITgcm model (Marshall et al. (1997)) was set up in nonhydrostatic pressure mode to model the same canyon bathymetric geometry that was modeled in the IT-response paper (Zhang et al. (2014)). Test calculations with the extended Korteweg-de Vries model with rotation (eKdVf) showed that the climatological stratification used in the IT study was too weak to form nonlinear waves as they appear in Figure 1. The density gradient in the thermocline was therefore increased. This gradient was well within the range of observed conditions. For test purposes, the

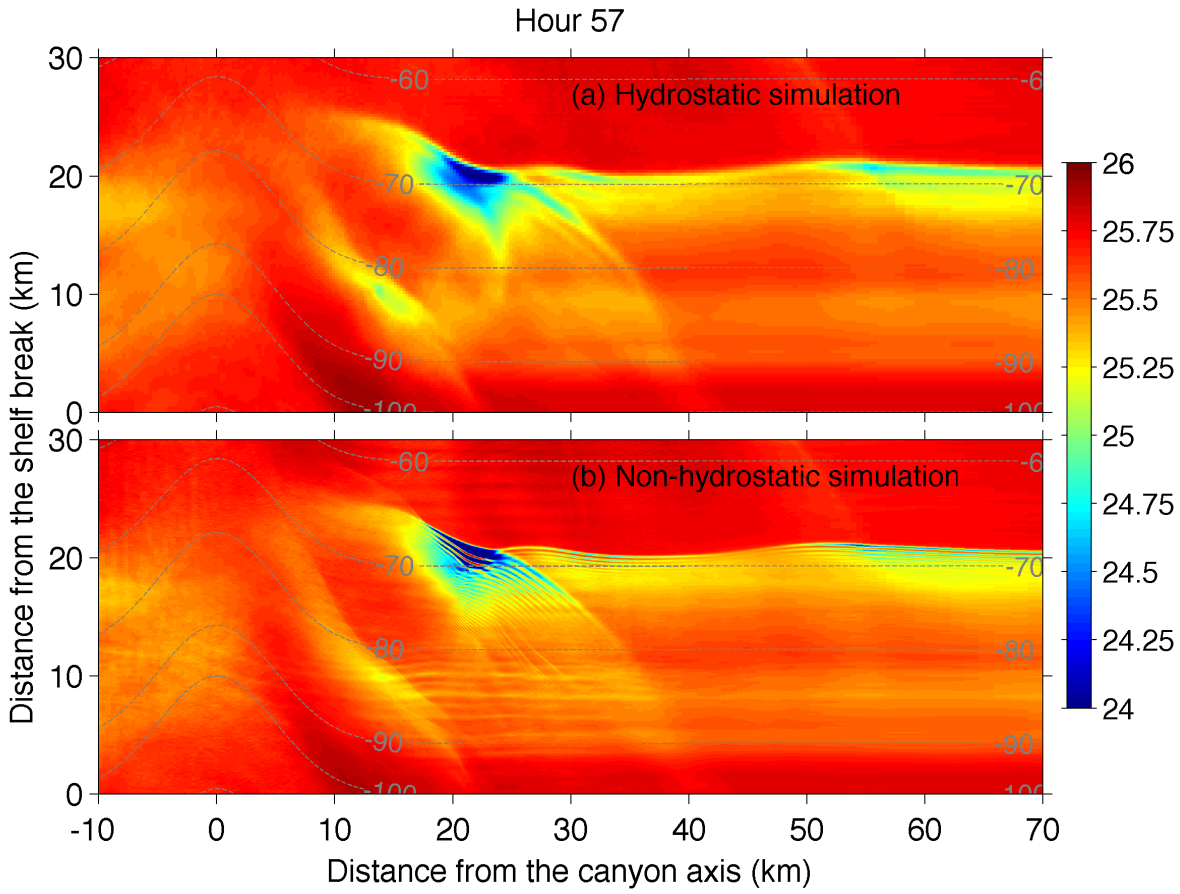

Figure 3: Time-snapshot simulation results are shown for flow near a canyon for the scenario of a barotropic M_2 tide incident from offshore (below). The density at 30-m depth is shown. Depth contours are shown (meters). The MITgcm primitive equation code is used. (a) Results for a simulation with the hydrostatic pressure assumption, which disallows short waves with nonhydrostatic pressure. (b) Results for a simulation including the nonhydrostatic pressure.

MITgcm was also run with the hydrostatic pressure constraint and relatively low horizontal resolution (250-m grid spacing), a far more rapid computation. As in the IT-response work, the maximum M_2-period tidal flow is subcritical, so that high-frequency lee waves are not generated at the slope. In contrast, the nonhydrostatic simulation employs close grid spacing, as fine as 25 m in the canyon area.

The computational result for the internal waves radiated from the action of a barotropic tide incident on a canyon is shown in Figure 3. Results with and without nonhydrostatic pressure are shown. The nonhydrostatic computation of six M_2 tidal periods required approximately 475,000 cpu hours. The nonhydrostatic simulation waves are shown at a slightly later moment in Figure 4 in a "synthetic" synthetic aperture radar format (a plot of the gradient of density at one level) with noise speckle added, which illustrates the variable grid spacing. In the main wave zone, three rounded internal-wave packets lie near each other, indicating multiple apparent internal-tide to nonlinear-wave conversion sites. A focussing point is seen for the internal tide, from which the nonlinear wave packets emerge in the nonhydrostatic simulation. Figure 5 shows slices through the waves of the two Fig 3. fields at $x = 21$ km. One notable result is that the leading edge of the wave is in almost the same position for the two cases. However, the multiple intersecting groups

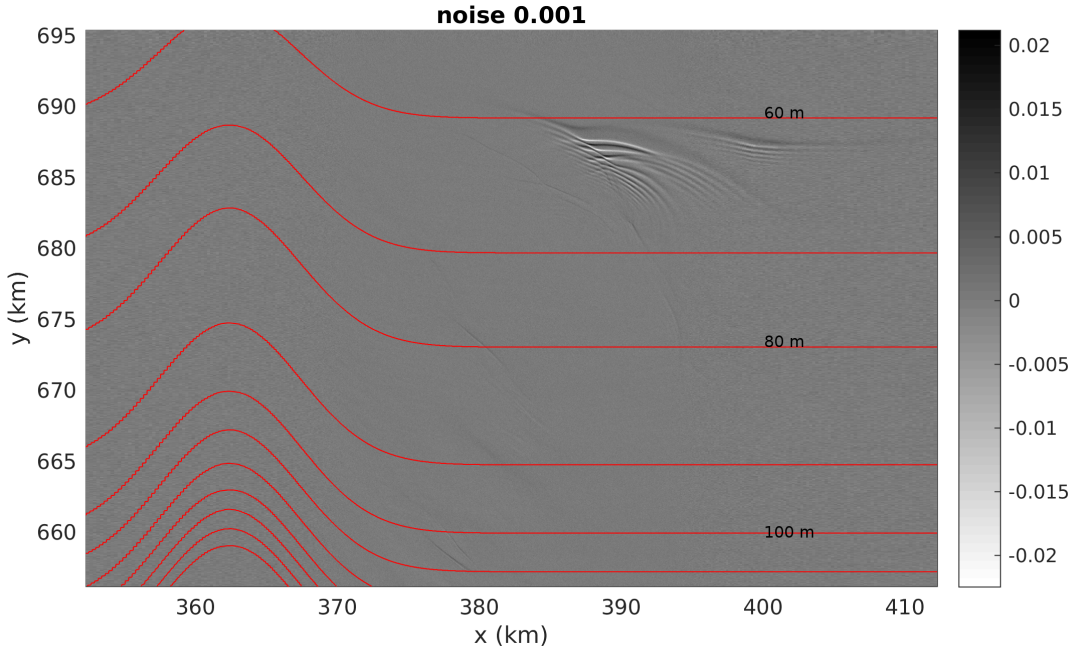

Figure 4: A synthetic SAR image of the waves seen in the Figure 3 nonhydrostatic frame is shown, for a slightly later moment in time. Bathymetric contours are shown at 10 meter interval.

of waves in the nonhydrostatic simulation output are not detectable in the hydrostatic simulation output.

4 Hybrid Model of the Wave Response

The hybrid model, presented in Duda et al. (2014), uses inputs from a hydrostatic computational model (HCM) to predict the nonlinear internal-wave response to barotropic tidal forcing over slopes such as the canyon using only a tiny fraction of the computational assets needed for the 3D nonhydrostatic computational simulation. The model is optionally data driven, if forecasts are desired instead of physical process studies. First, the HCM output is separated into a background state and time-dependent fluctuations within a moving time window. The mode-one internal tide wave speed, with current effects included so that is is anisotropic, is then computed throughout the domain to be used for internal-tide ray tracing. Initial ray directions near the critical slope locus (for slopes that are supercritical at maximum steepness, steeper than internal-wave characteristics at the chosen tidal frequency, as they are throughout this paper) are determined by tidal analysis of the residual time-varying field, and then using a correlation method to fit local plane waves. After rays are traced from multiple along-slope positions, the regularized extended Korteweg-de Vries model with rotation (Holloway et al. (1999)) is then solved along the rays to produce the short-wavelength (nonhydrostatic) internal waves. The full three-dimensional field can be estimated by interpolating between adjacent rays. A result is shown in Figure 5, which does not show the interpolation step. It can be seen that packets of nonlinear waves develop on the right-hand side of the canyon (look up the canyon) but not on the left-hand side, as in the primitive equation results. This result is obtained in a small fraction of the time needed for the direct numerical result (Figure

3).This method breaks down when rays cross, but it provides a rapid way to compute approximate wave positions and amplitudes as a function of time in a data-driven context. with the major computation being the 4D HCM.

The work illustrates the importance of a few unanswered research questions. One of them is the conversion of a beam of tidal energy radiating upward from a critical slope zone (as shown in Zhang et al. (2014)) into a largely mode-one internal wave field as is commonly observed. The fact that this is unanswered becomes evident when extracting eKdVf initial conditions from the internal-tide output of the HCM. If the output is filtered to yield mode-one energy, the mode coefficients (the dependent variable of the eKdVf) are small (weak waves) that do not steepen into nonlinear wave packets. Instead, if the mean displacement over the lower-half of the used to calculate the initial conditions, the results more closely match the primitive equation results. Is it evident that almost all of the internal-wave energy moves into the mode-one internal tides while propagating upslope, even though the energy initially scatters between multiple modes near the generation zone, but the mechanism for this has not been fully described.

5 Summary

We have simulated the formation of isolated packets of nonlinear internal waves, formed from tidal-frequency internal waves, at one side of a canyon, using a primitive equation model that includes nonhydrostatic pressure. A simulation with hydrostatic pressure produces distorted wide waves in place of the packets, with the leading edge at the correct position, possibly close enough to mark the location of the wave packets. The similarity of the two results suggests that the initial stages of packet formation can be modeled with useful accuracy with hydrostatic simulations, possibly allowing packet position forecasting. Position forecasting may be useful during some at-sea operations, for example for acoustic prediction purposes.

A hybrid or composite modeling approach that uses output from the hydrostatic simulation also shows packet formation on one side of the canyon. This model has not yet been modified to take into account energy changes caused by ray divergence, but it nonetheless shows nonlinear waves primarily on one side of canyon, as with the nonhydrostatic simulation. The accuracy of this approach has not yet been evaluated by comparison with the nonhydrostatic simulation. The situation of crossing internal-tide rays is not well handled by the composite model, compromising its usefulness in areas of ray focusing which are common around the canyon.

Acknowledgments: This work was supported by Office of Naval Research (ONR) MURI Grant N00014-11-1-0701. DoD HPC resources were used for the nonhydrostatic simulation.

References

Baines, P. G. (1982). On internal tide generation models. *Deep-Sea Res.*, 29:307–338.

Duda, T. F., Zhang, W. G., Helfrich, K. R., Newhall, A. E., Lin, Y.-T., Lynch, J. F., Lermusiaux, P. F. J., Haley, Jr., P. J., and Wilkin, J. (2014). Issues and progress in the prediction of ocean submesoscale features and internal waves. In *Oceans '14 St. John's Conference Proceedings*. IEEE/MTS.

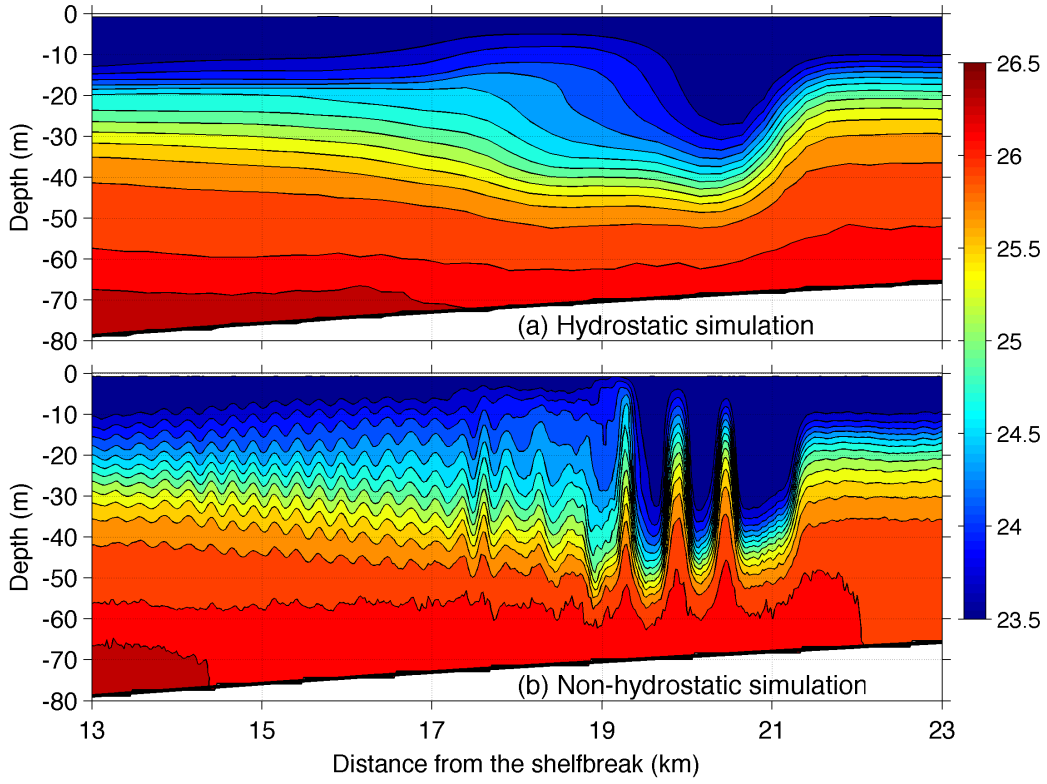

Figure 5: Slices of density at $x = 21$ km from the outputs depicted in Figure 3 are shown.

Garrett, C. and Kunze, E. (2007). Internal tide generation in the deep ocean. *Ann. Rev. Fluid Mech.*, 39:57–87.

Holloway, P. E., Pelinovsky, E., and Talipova, T. (1999). A generalized Korteweg-de Vries model of internal tide transformation in the coastal zone. *Journal of Geophysical Research: Oceans*, 104(C8):18333–18350.

Jackson, C. R. (2004). *An Atlas of Internal Solitary-like Waves and Their Properties*. Global Ocean Assoc., Alexandria, VA, second edition.

Li, Q. and Farmer, D. M. (2011). The generation and evolution of nonlinear internal waves in the deep basin of the South China Sea. *J. Phys. Oceanogr.*, 41(7):1345–1363.

Marshall, J., Adcroft, A., Hill, C., Perelman, L., and Heisey, C. (1997). A finite-volume, incompressible navierstokes model for studies of the ocean on parallel computers. *J. Geophys. Res.*, 102:57535766.

Schiff, L. I. (1968). *Quantum Mechanics*. McGraw-Hill Book Company, New York.

Shchepetkin, A. F. and McWilliams, J. C. (2005). The regional oceanic modeling system (roms): A split-explicit, free-surface, topography-following-coordinate oceanic model. *Ocean Modell.*, 9:347404.

Zhang, W. G., Duda, T. F., and Udovydchenkov, I. A. (2014). Modeling and analysis of internal-tide generation and beamlike onshore propagation in the vicinity of shelfbreak canyons. *J. Phys. Oceanogr.*, 44(3):834–849.

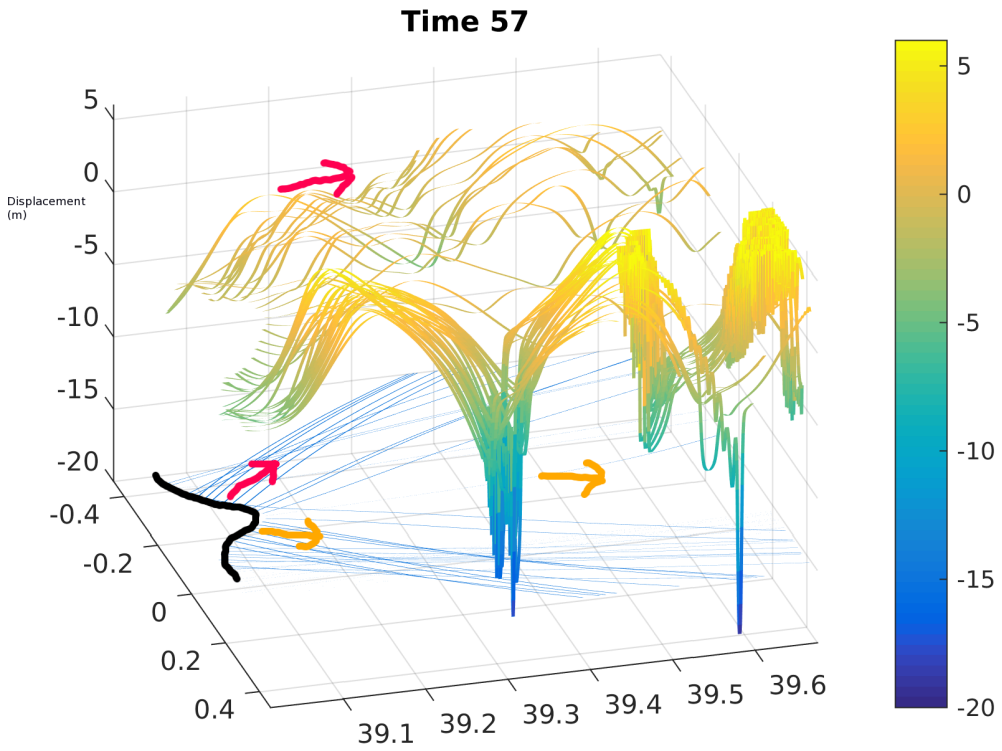

Figure 6: A snapshot of mode-one wave amplitudes computed with the Korteweg-DeVries type wave evolution model is shown along internal-tide rays computed from ROMS model output. Pseudo latitude and longitude are used here, consistent with the rotation of the simulation. One isobath at the canyon is shown in black. The arrows show the directions of internal wave propagation.